Chapter 16

Temporal Dynamics of Spontaneous Ca^{2+} Transients, ERBB4, vGLUT1, GAD1, Connexin, and Pannexin Genes in Early Stages of Human Stem Cell Neurodifferentiation

Pallavi V. Limaye, Michele L. McGovern,
Mandakini B. Singh, Katerina D. Oikonomou,
Glenn S. Belinsky, Erika Pedrosa,
Herbert M. Lachman and Srdjan D. Antic

Additional information is available at the end of the chapter

http://dx.doi.org/10.5772/62769

Abstract

Spontaneous Ca^{2+} transients drive stem cell proliferation and neurodifferentiation. Deciphering the relationship between neuronal and glial human genes on one side and spontaneous Ca^{2+} activity on the other side is essential for our understanding of normal brain development, and for insights into the pathogenesis of neurodegenerative and neurodevelopmental disorders. In the present study, forebrain neurons were derived from human embryonic and induced pluripotent stem cells (hESC-H9 and iPSC-15; 22q11.2 deletion) over a period of 21 days in vitro (DIV). Every 1–2 days, multisite optical imaging technique was applied to detect populations of cells with spontaneous Ca^{2+} transients. The expression levels of 14 genes of interest were analyzed by quantitative polymerase chain reaction (qPCR) on the same biological samples where physiological recordings were performed. The genes analyzed include: the schizophrenia candidate gene *ERBB4*, connexin (*Cx*) genes *Cx26, Cx36, Cx43, Cx45, Cx47*, pannexin-1 (*PNX1*), neuronal markers *PAX6, vGLUT1, GAD1, TUBB3*, glial lineage markers *BLBP, GFAP*, and housekeeping gene *ACTB*. We found that Ca^{2+} signals decrease in amplitude, decrease in duration, and increase in frequency during the first 21 days of human neurodifferentiation. The expression levels of *ERBB4, PAX6, GAD1, vGLUT1, BLBP, Cx36, Cx45*, and *PNX1* were found to be strongly positively correlated with the percentage of cells exhibiting spontaneous Ca^{2+} transients ("Active Cells"). While expression of *BLBP, Cx45, ERBB4, GAD1, PAX6, PNX1*, and *vGLUT1* were correlated with short-duration and long-amplitude Ca^{2+} transients, *Cx43, TUBB3*, and *Cx47* were better correlated with long-duration and short-amplitude transients. The expression dynamics of *Cx26* was unrelated to any aspect of spontaneous Ca^{2+} activity. Four genes showed an exponential time course

with a distinct onset on a given DIV. The onset of *PNX1, ERBB4*, and *vGLUT1* occurred before, while the onset of *Cx36* occurred after the first action potentials were detected in early differentiating human neurons.

Keywords: embryonic, induced pluripotent, spontaneous activity, Ca^{2+} imaging, schizophrenia, action potential

1. Introduction

Deciphering human brain development requires the understanding of physiological processes of neuron progenitors and differentiating neurons [1–3]. Although electrical and optical recordings from postmitotic human neurons can be achieved using acute human fetal brain slices [4,5], the overwhelming majority of studies on the physiology of postmitotic human neurons use human embryonic or induced pluripotent stem cells [6–12]. The implementation of human stem cell technologies brings two advantages:

1. Culturing of human neurons alleviates severe ethical and technical limitations associated with physiological recording in fetal brain slices.
2. In vitro differentiation of human neurons underlies state-of-the-art experimental models of neurodegenerative disorders [13–15].

Much of the current research effort on stem cell-derived human neurons is focused on the gene expression levels, but it is also necessary to elucidate physiological signals that either drive genes, or are driven by genes. Among these signals are transient changes in intracellular Ca^{2+} concentration [16–19].

Spontaneous Ca^{2+} transients are detected in the developing cortex before the input of sensory information [20]. In the earliest stages of neurogenesis, Ca^{2+} transients control fundamental cell processes such as proliferation, migration, and differentiation of neural progenitors into neurons [2,21,22]. Spontaneous Ca^{2+} transients differ in characteristics such as duration, frequency, and amplitude, encoding information that can be decoded by proteins within the cell, thus allowing the latter to exert control over various processes. High-frequency Ca^{2+} oscillations trigger events such as the release of neurotransmitters, whereas low-frequency activity is indicative of slower processes such as gene transcription [23].

Given the interdependence between Ca^{2+} signals and the gene transcription process, we hypothesized that the expression levels of a particular human gene may correlate with the onset of a particular type of Ca^{2+} activity in differentiating cells. This working hypothesis is bidirectional. On one hand, a gene may code for proteins that bring Ca^{2+} into the cells, in which case an increase in gene expression changes the pattern of ongoing Ca^{2+} transients. On the other hand, if Ca^{2+} activity activates gene transcription, mRNA levels will rise in the cytosol in response to a certain amplitude, duration, or frequency of spontaneous Ca^{2+} transients. In order to test for possible correlations between Ca^{2+} activity and gene expression levels, forebrain neurons were derived from human stem cells over 21 days in vitro (DIV). At regular time

http://dx.doi.org/10.5772/62769

intervals (every 2 days), the patterns of spontaneous Ca^{2+} signaling were recorded optically using a Ca^{2+}-sensitive dye. Multisite Ca^{2+} imaging allowed us to determine the duration, frequency, and amplitude of spontaneous Ca^{2+} transients at each DIV. The physiological measurements were followed by gene expression analysis on the same in vitro samples (cell cultures) in which physiological recordings were made. We experimented with hESC and iPSC technologies in order to study the physiological activity and gene expression during the earliest stages of human neurodifferentiation, when pluripotent cells transition into neuron progenitors, which in turn transition further to postmitotic neurons. The following 14 genes were examined: the schizophrenia candidate gene *ERBB4;* neuronal markers: *PAX6*, *vGLUT1*, *GAD1*, *TUBB3*; the glial lineage markers *BLBP* and *GFAP;* several connexins (*Cx26*, *Cx36*, *Cx43*, *Cx*45, *Cx47*); a pannexin (*PNX1*); and the housekeeping gene *ACTB*. We found that Ca^{2+} transients with specific temporal properties are significantly correlated to the expression of a select group of genes during these early stages of neuronal development.

2. Materials and method

2.1. Cell lines

Human embryonic stem cell line (hESC-H9) was obtained from the University of Connecticut Stem Cell Core. The induced pluripotent stem cell line (iPSC-15, 22q11.2 deletion, passages 11–14, in [24] called SZ22del15-6) was created at the Albert Einstein College of Medicine (Bronx, New York). Both cell lines have also been used in a previous report [8], where it has been demonstrated that there is no difference in spontaneous activity or expression of selected genes between these two lines.

2.1.1. Differentiation protocol

Stem cell lines were differentiated using a five-stage protocol (**Figure 1A**) with defined media constituents [6, 25]. This protocol does not use typical brain region morphogens in Stages IV–V (besides those present in B27), and so is associated with the default production of forebrain neurons [26]. Briefly, stem cell colonies (Stage I) were dissociated by collagenase, and stem cell aggregates were incubated for 4 days in stem cell (SC) media without bFGF on ultralow adherence plates (Costar, Wilkes Barre, PA) (Stage II). 5 μM dorsomorphin (Chemdea, Ridgewood, NJ) and 5 μM SB431542 (Ascent, Princeton, NJ) were added to the media from days 1–8. Stem cell aggregates were then seeded on dishes coated with 1:100 Geltrex and allowed to expand for 4–8 days in NEP (neuroepithelial)–basal medium (Stage III) until neuroepithelial colonies appeared. NEP-basal medium consisted of DMEM/F12, 1 mg/ml BSA (Sigma), 1× N2, 1× B27 supplements without retinoic acid, and 1× penicillin/streptomycin/antimycotic. Thirty minutes before selecting the resultant neuroepithelial colonies, 0.66 mg/ml ROCK inhibitor (Y27632, Wako USA, Richmond, VA) was added to the media. Colonies with neuroepithelial morphology were removed by trituration and seeded with 0.66 mg/ml ROCK inhibitor on glass cover slips coated with 1:100 Geltrex. Cells were grown in NEP-basal medium with 20 ng/ml basic fibroblast growth factor (bFGF) for 7 days (Stage IV). Cells were

then maintained in NEP-basal medium in the presence of 10 ng/ml BDNF (brain-derived neurotrophic factor) (Peprotech, Rocky Hill, NJ) and 10 ng/ml GDNF (glial cell line-derived neurotrophic factor) (Peprotech) (Differentiation Stage V and maintenance). Media were changed every other day.

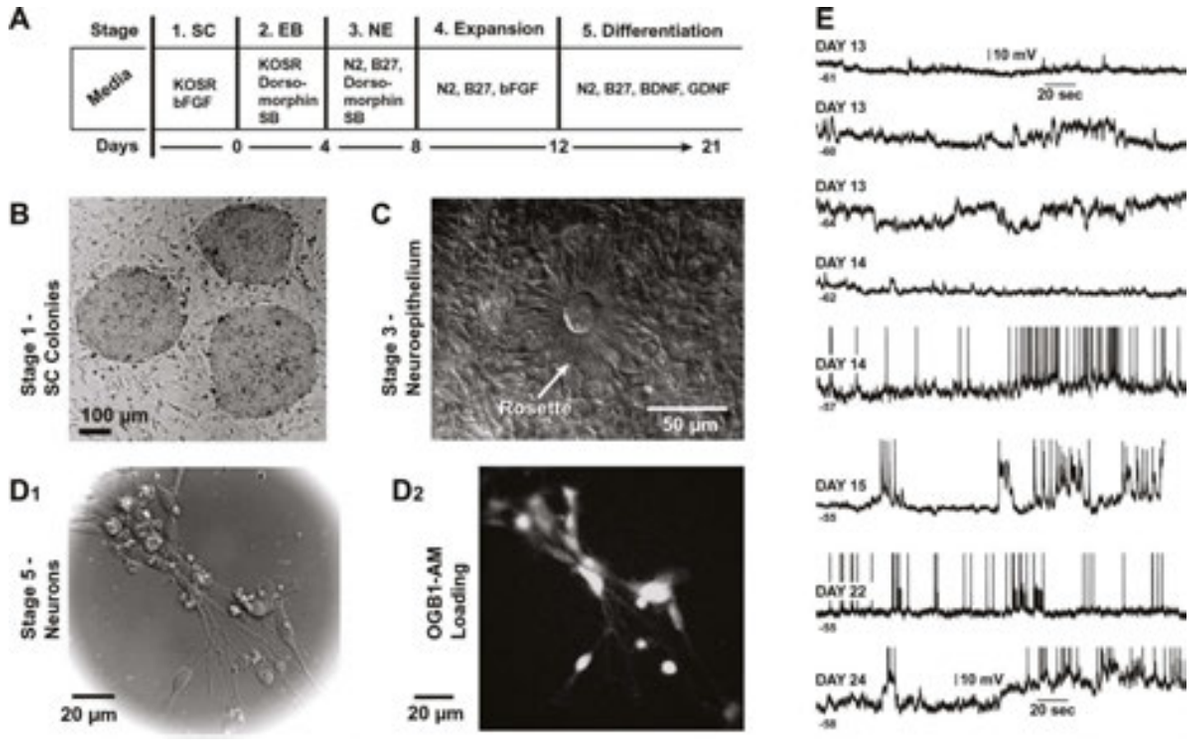

Figure 1. Human stem cell neurodifferentiation. (**A**) Timeline of the differentiation protocol comprising five stages. SC, induced pluripotent or embryonic stem cells; EB, embryoid bodies; NE, neuroepithelial colonies. (**B**) Dark-field photograph of undifferentiated stem cell colonies. (**C**) IR DIC photograph of the neuroepithelium with formed rosettes Stage III. ($\mathbf{D_1}$) IR DIC photograph of postmitotic neurons—Stage V. ($\mathbf{D_2}$) The same neurons as in $\boldsymbol{D_1}$, loaded with OGB1-AM and photographed in the fluorescence channel (excitation, 470 nm). (**E**) Whole-cell recordings of spontaneous electrical activity from cultured cells on DIV-13 to DIV-24. Resting membrane potential shown under the trace. Action potentials are truncated for clarity.

2.1.2. Electrophysiology

Whole-cell patch recordings were performed as previously described [6]. Briefly, before recordings, cells were transferred to an Olympus (Tokyo, Japan) BX51WI upright microscope (equipped with infrared video microscopy) and incubated in DMEM/F12, 0.075% BSA, 0.25× B27, Pen/Strep/Antimycotic, and 14 mM HEPES, pH 7.4. Individual cells were selected for recordings based on a small round or ovoid cell body (diameters, 5–10 μm) and typically two or more extended processes. Pipettes (10 MΩ) were filled with an intracellular solution containing (in mM) 135 K-glutamate, 10 HEPES, 2 $MgCl_2$, 3 ATP-Na_2, 0.3 GTPNa_2, and 10 P-creatine Na_2, pH 7.3. Recordings were performed using Multiclamp 700B and Clampex9.2 (Molecular Devices, Union City, CA). In the current clamp configuration, we measured the resting membrane potential, and then a negative holding direct current (in the range −2 pA to

http://dx.doi.org/10.5772/62769

−15 pA) was applied to bring the membrane potential to approximately −60 mV. This was done to compare neurons under identical conditions during spontaneous activity. Spontaneous activity was monitored for 5 min continuously. Electrical traces were analyzed using Clampfit 9.2 (Molecular Devices).

2.2. Ca^{2+} imaging

Multisite Ca^{2+} imaging was used to record spontaneous activity in cells cultured on glass cover slips (12 mm). The cells were loaded with a Ca^{2+}-sensitive fluorescent dye by incubating the cover slips for 30 min with membrane-permeable Oregon Green 488 Bapta-1-AM (OGB1-AM, Invitrogen 06807) at 37°C. The cells were then washed with warmed media and allowed to recover for additional 30 min in the incubator (37°C). Cover slips were placed in the recording chamber and perfused with modified Krebs-Ringer solution. Images were projected onto an 80 × 80 pixel CCD camera (NeuroCCD-SMQ, RedShirtImaging, Decatur, GA) and sampled at 800 ms/frame. One to four nonoverlapping visual fields were sampled per cover slip. The cells were then frozen and kept at −80°C until RNA extraction. Analysis of optical signals was done off-line using Neuroplex software (RedShirtImaging). The following definitions were applied for the analysis of data obtained by multisite Ca^{2+} imaging:

Active Cells: In each visual field, the number of cells showing at least one Ca^{2+} transient was divided by the total number of cells in that field (%).

Repetitive Activity: The number of cells in the visual field exhibiting four or more Ca^{2+} transients per 5 min of optical recording, divided by the number of "Active Cells" (cells showing at least one Ca^{2+} transient) in that field (%).

Amplitude of a Ca^{2+} transient was measured from the baseline before the signal onset to the signal peak, and expressed as $\Delta F/F$ (%).

Duration of the Ca^{2+} transient was measured at half amplitude (half-width) and expressed in seconds. The median of duration of all recorded Ca^{2+} signals (n = 4744) was determined to be at 8 s. Ca^{2+} signals were then separated into two groups, one consisting of "wide" and the other of "narrow" events. *Wide*: An event endowed with a half-width longer than 8 s. *Narrow*: An event was considered to be narrow if the duration (measured at half amplitude) was less than or equal to 8 s.

2.3. RNA extraction

The samples were removed from −80°C, and 300 μl of Trizol was added to each well containing a cover slip. Cells were detached from the cover slips by rinsing with Trizol. The cover slips were then discarded and 1 μl of yeast tRNA 10 μg/μl (Sigma) was added to each well. The cells were allowed to sit for 2 min at room temperature; then they were triturated, and the contents from each well were transferred to a separate 0.5 ml microcentrifuge tube. A volume of 60 μl of chloroform was added to each sample and shaken vigorously for 15 s. The tubes were incubated at room temperature for 15 min and were then centrifuged at 12,000 g for 15 min at 4°C. They were then placed on ice, and the clear, aqueous phase from each tube was

removed and transferred to a new 0.5 ml microcentrifuge tube.150 μl of 100% isopropanol was then added to each sample. The contents of each tube were mixed, allowed to rest for 10 min at room temperature, and then centrifuged at 12,000 g for 10 min at 4°C. An RNA pellet was located in each tube and the supernatant removed. 0.3 ml of cold 75% ethanol was added to each tube, which was then vortexed and centrifuged at 7,500 g for 5 min at 4°C.The supernatant was again removed and the pellets allowed to air-dry. The pellets were then resuspended in 7 μl of RNase-free water and incubated at 55°C for 10 min, using the PCR machine (Eppendorf Mastercycler Gradient, Hauppauge, NY). In order to remove any genomic DNA contamination, samples were subjected to treatment with DNase according to the manufacturer's protocol (New England Biolabs).

2.4. cDNA synthesis

The following were mixed: 5 μl RNA, 0.75 μl of mixed OligodT and Random Hexamers 1:1 (Qiagen, Valencia, CA), 1 μl (10 mM each) dNTPs (Promega, Madision, WI), and 3.25 μl RNase-free water (Invitrogen). There was also an NTC (no template control) tube which contained 5 μl of RNase-free water in place of RNA. The reagents in each tube were mixed thoroughly and placed in the PCR machine with a preheated lid of 80°C. The samples were incubated at 65°C for 5 min and then immediately placed on ice (for at least 1 min). 4 μl of 5× SuperScriptIII Buffer (Invitrogen), 1 μl DTT (Invitrogen), 1 μl RNaseOut (Invitrogen), 3 μl DNase-free water, and 1 μl SuperScriptIII (Invitrogen) were added to the 10 μl already present in each tube. 4 μl 5× SuperScriptIII buffer, 1 μl DTT, 1 μl RNaseOut, and 4 μl DNase-free water were added to −RT (No Reverse Transcriptase) tubes. The reagents in each tube were mixed thoroughly and placed in the PCR machine at 25°C for 5 min, 37°C for 10 min, 50°C for 80 min, and 70°C for 15 min. The samples were then stored at −20°C. For positive controls, total RNA of human fetal brain (Clontech, Mountain View, CA) was used.

2.5. Preamplification

Primer pools of long outer primers were made in water, 1 μM each for up to 14 genes in total. The following reagents were mixed for 80 μl pre-amp reactions: 16 μl 5× GoTaq Flexi Buffer Colorless (Promega), 4.8 μl of 25 mM $MgCl_2$, 1.6 μl of 10 mM dNTPs, 3.2 μl primer pool, 1.28 μl GoTaq DNA polymerase (Promega), 48.12 μl water, and 5 μl cDNA. The lid of the Eppendorf Mastercycler Gradient was preheated to 104°C, and the pre-amplification PCR was run at 94°C—4 min [94°C—30 s, 55°C—30 s, 72°C—40 s] for 10 cycles, and 72°C—10 min.

2.6. Quantitative polymerase chain reaction (qPCR)

qPCR was performed on the genes of interest by mixing the following reagents: 3 μl 5× PCR buffer, 0.9 μl 25 mM $MgCl_2$, 0.5 μl 10mM dNTPs, 1 μl 10 μM mixed forward and reverse primers (**Table 1**), 0.75 μl 10 μM FAM BHQ Probe (Sigma), 0.4 μl GoTaq, 5 μl preamplified cDNA, and 13.45 μl water. The final volume in each well was 25 μl. qPCR was performed using the Bio-Rad CFX Connect Real-Time PCR Detection System. Samples were run at 94°C—3 min, [94°C—30 s, 55°C—30 s, 72°C—30 s] for 40 cycles, with the annealing temperature dependent on the primers. **Table 1** shows screened nested primers, probe sets, and the

http://dx.doi.org/10.5772/62769

annealing temperatures. Gene expression data were normalized using housekeeping gene *ACTB* as a reference, using the 2-ΔΔCt method.

2.6.1. Data sets

In the present study, spontaneous Ca^{2+} activity was recorded in 25 cultures containing developing human neurons at various ages (differentiation days: 7, 8, 9, 10, 11, 14, 15,16, 17, 18, and 21). Ten cultures were from iPSC-15 and 15 cultures contained hESC-H9 cells (**Table 2A**). The total number of spontaneous Ca^{2+} signals analyzed from Day 7 to Day 21 is 4744. All 25 cultures were saved after the recording session and subjected to gene expression analysis. In addition to these 25 cultures, the identical gene analysis was performed on 23 cultures in which recordings were not performed (**Table 2B**). No significant differences in gene expression levels of 14 genes (see list above) were detected between recorded and nonrecorded cultures (data not shown); hence, the gene expression data from recorded and nonrecorded cultures were combined. The gene expression data from DIV 8 to DIV 21 were used in the "gene-to-gene" correlation analyses (N = 45 cultures/cover slips). The physiological and gene expression data from DIV 7 to DIV 21 were used in the activity-to-gene correlation analyses (n = 4744 calcium transients, N = 48 cultures).

Gene	Outer primers 5′–3′ forward; reverse (annealing temperature)
	Inner primers 5′–3′, forward; reverse (annealing temperature)
	Probe
ACTB	CCTCGCCTTTGCCGATCC; GATGCCGTGCTCGATGGGGT (55°C)
	CCTCGCCTTTGCCGATCC; GCGAAGCCGGCCTTGCACAT (55°C)
	famATGATATCGCCGCGCTCGTCGTCGAbhq
TUBB3	ACTCCCTTGAACAGGGACAGGGA; GTTCCGGGTTCCAGGTCCACCA (55°C)
	CACAGGCGTCCACAGTTCT; CGAGTCGCCCACGTAGTTG (55°C)
	famCATCAGTGATGAGCATGGCATCGACCbhq
ERBB4	GGAGTACTTGGTCCCTCAGGCT; GGGTGCCACTGGCTTGCGTA (55°C)
	GCAAGAATTGACTCGAATA; CTGGAATTGTGCTAGTTG (50°C)
	famCAGACACTCCTTGTTCAGCAGCbhq
GAD1	GATGATGGGCGTGCTGTTGC; GCGGCTGGGTTGGAGATGAC (55°C)
	CGACACCGGGGACAAGGCAATT; CCGTCGTTGAGGGCTGTCTGG (55°C)
	famCAATGGCGAGCCTGAGCACACAAACGTCTGbhq
vGLUT1	CGCTACATTATCGCCATCATGAG; GGTGGGGCCCATTTGCTCCA (55°C)
	CAGGAGGATTTATCTGTCAAAAAT; GGGTATGTGACCCCCTCTACCAAC (55°C)
	famATGCTGATCCCCTCAGCTGCCCGCbhq
PAX6	AGCCCAGTATAAGCGGGAGTGC; TCCCCCTCCTTCCTGTTGCTGG (55°C)

	TCTTTGCTTGGGAAATCCG; CTGCCCGTTCAACATCCTTAG (55°C)
	famTCATACATGCCGTCTGCGCCCATCTGbhq
PNX1	CGCTGTTTGTTCCATTCCGAC; TCTCTGTCGGGCATTCTTCTC (55°C)
	GGAGAATATTAAGAGCAGTGGTC; CTGTCTATGTTCATACCTTGGAG (45°C)
	famCGACCCAATGCTACTCCTGACAAACCTbhq
CX26	TCCCGACGCAGAGCAAAC; GCAGGGTGTTGCAGACAAAG (55°C)
	TCCCGACGCAGAGCAAAC; AGGGTGTTGCAGACAAAGTC (55°C)
	famCCCACACCTCCTTTGCAGCCACAbhq
CX36	GCAGCACTCCACTATGATCGG; GGAAGACCCAGTAACGTATGTG (55°C)
	ACTCCACTATGATCGGGAGGATCC; CTGCAGGGTGTTGCACAC (53°C)
	famCTGCTCATCATCGTACACCGTCTCCCCbhq
CX43	AGGAGTTCAATCACTTGGCG; GTACTGACAGCCACACCTTC (55°C)
	CTTGGCGTGACTTCACTAC; GCAGTTGAGTAGGCTTGAAC (55°C)
	famCGCTCCAGTCACCCATGTTGCCTGbhq
CX45	TGGACAACAGGGCATACC; GCAAACGCATCATAACAGAC (55°C)
	TGGACAACAGGGCATACC; CGGAAGACAATCAGAACAGTG (55°C)
	famAGTTGGAGCTTCCTGACTCGCCTGCbhq
CX47	CCCAGGACAATCAGGGATTC; CAGGCCAGAAAATTCCAGTC (55°C)
	CAGGACAATCAGGGATTC; CCAGAAAATTCCAGTCTCC (51°C)
	famCTGCTTGGATGCTGGTCCTCCbhq
BLBP	GGTGGGAAATGTGACCAAAC; TGTCTCCATCCAGGCTAACA (55°C)
	CAACGGTAATTATCAGTCAAG; GGCTAACAACAGACTTACA (51°C)
	famTCATCAGGACTCTCAGCACATTCAAbhq
GFAP	CTGCGGCTCGATCAACTCA; GTAGTCGTTGGCTTCGTGCT (55°C)
	GCCTATAGACAGGAAGCA; GTGGATCTTCCTCAAGAAC (49°C)
	famCCTCCAGCGACTCAATCTTCCTbhq

Annealing temperatures for standard three-step PCR are included.

Table 1. Screened nested primer and probe sets designed to amplify mRNA without amplifying genomic DNA.

2.7. Statistical analysis

Statistical analysis was performed using SigmaStat 2.03 (Systat, San Jose, CA). Data are presented as mean ± SEM. Statistical differences between the groups were evaluated with Student's *t*-test for paired data. Pearson's product–moment correlation coefficient was used to determine the correlation between gene expression levels and spontaneous activity. Unavailable values from DIV 7 to DIV 21 were interpolated from the original data set using

http://dx.doi.org/10.5772/62769

the method of Least Squares Fit (n = 15, where n = number of DIV; df = 13, where $df = n - 2$). Only values with $p < 0.001$ ($r \geq 0.76$) were considered statistically significant. For "gene-to-gene" correlation analyses, n = 12, where n = number of DIV, and df = 10, where $df = n - 2$). DIV 7 was not included in these correlation analyses.

3. Results

3.1. Stem cell-derived human neurons

Two human stem cell lines (hESC-H9 and iPSC-15) were subjected to a five-stage neurodifferentiation protocol over a period of 21 days (**Figure 1A**). The first stage (Stage I) was used to grow and maintain undifferentiated stem cell colonies (**Figure 1B**). Day 0 (DIV 0) marks the Seeding of embryoid bodies. Upon seeding, the cells from the embryoid bodies begin to form neuroepithelial structures (**Figure 1C**, Rosettes). The neuroepithelial cells were expanded in a bFGF-rich media for 4 days (Stage IV). The expanded NEs were lifted on DIV 12 and re-seeded on glass cover slips in BDNF/GDNF-based neurodifferentiation media (Stage V). This protocol produced cells with neuronal morphologies (**Figure 1**D_1) and neuronal electrical properties, namely the ability to fire action potentials. Whole-cell recordings were performed on cells with a neuronal appearance—cells with processes visible in IR DIC microscopy (**Figure 1**D_1). That is to say that sampling of cells for electrical recordings was biased by visual appearance. The first action potentials were detected on DIV 14, n = 3 (n = number of cells) (**Figure 1E**). During the fifth stage (Stage V), whole-cell recordings revealed that some, not all, stem cell-derived neurons were spontaneously producing bursts of action potentials.

In our previous study, stem cell-derived human neurons were grown for 88 days, characterized electrophysiologically, and individual cells were captured for gene expression analysis [8]. The previous study, which used the same two stem cell lines under an identical five-stage differentiation protocol and systematic whole-cell recordings (n = 229 human cells from Day 13 to Day 88) produced detailed distributions of electrophysiological properties [8, supplemental figure S1]. In the present study, the focus is on the first 21 days of stem cell neurodifferentiation, when pluripotent stem cells transition to neural progenitors and when first postmitotic neurons are born. Also, in the present study, the gene analysis was performed on the whole population of cells, unbiased by visual appearance or physiological recordings; hence, all cell types present in the culture were included in the RNA samples.

3.2. Spontaneous Ca^{2+} transients

Every 1–2 days, glass cover slips containing cultured human cells were removed from the incubator, loaded with a Ca^{2+}-sensitive dye OGB1-AM, and positioned in the recording chamber of the electrophysiological imaging station (**Figure 1**D_2). Multisite optical recordings of unprovoked (spontaneous) Ca^{2+} activity were performed from DIV 7 to DIV 21 in 136 locations (visual fields, **Figure 2A**$_1$) distributed across 25 cover slips (one visual field approximately 380 × 380 μm^2). Regions of interest (ROIs) were placed on all OGB1-stained cells, indiscriminately (**Figure 2A**$_2$). Therefore, the ROIs include both neurons and nonneurons

present in the culture. From each visual field, the Ca^{2+} signals were recorded for at least 5 min (**Figure 2B**). In the majority of visual fields, three successive optical recording trials were performed, extending the total monitoring to 15 min. Long recording sessions were needed, because spontaneous outbursts of electrical activity in developing human neurons are interspersed by silent periods that may last for several minutes [5]. Cells were deemed "active" if at least one Ca^{2+} transient was detected (**Figure 2B**, upper traces). Some cells showed no activity throughout the entire recording sessions (**Figure 2B**, lower traces). The percentage of

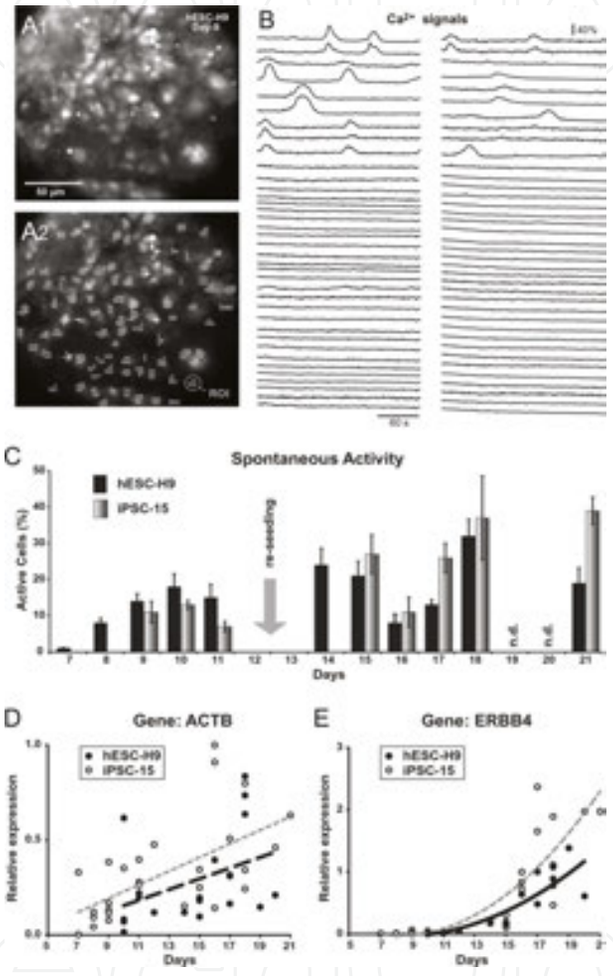

Figure 2. Two human lines (hESC-H9 and iPSC-15) produce cells with similar Ca^{2+} activity and gene expression. (**A_1**) hESC-H9 cells on DIV-9 were bulk-loaded with OGB1-AM. Image captured by fast data acquisition camera (80 × 80 pixels). (**A_2**) Same as in A_1, except gray dashes mark the actual pixels used to generate regions of interest (ROI). (**B**) Spontaneous Ca^{2+} transients from 75 ROIs are shown. Each trace represents 3.5 min of continuous optical monitoring. Cells with spontaneous Ca^{2+} activity, "Active Cells," are grouped on the top. The majority of ROIs have no spontaneous Ca^{2+} transients. (**C**) The average "Active Cells" per day of differentiation for two stem cell lines, hESC-H9 (black) and iPSC-15 (gray). "Active Cells": the number of ROIs with Ca^{2+} transients divided by the total number of ROIs in the visual field. Error bars are s.e.m. The number of visual fields studied by multisite Ca^{2+} imaging in the two stem cell lines on each DIV are listed in **Table 2A**. On DIV-12, the expanding colonies were lifted and reseeded on fresh cover slips in a new type of a differentiation media (addition of BDNF and GDNF). (**D**) Gene expression of ACTB measured in the hESC-H9 (black) and iPSC-15 line (white). Each data point represents one cover slip (one culture). Black and gray trend lines are polynomial fits through the hESC-H9 and iPSC-15 data sets, respectively. (**E**) ERBB4 expression in two stem cell lines normalized to that of ACTB.

http://dx.doi.org/10.5772/62769

cells displaying spontaneous Ca^{2+} activity ("Active Cells") was calculated for each visual field by dividing the number of active ROIs (cells with Ca^{2+} signals) with the total number of ROIs in the visual field (**Figure 2A**$_2$). The average percentage of cells displaying spontaneous Ca^{2+} activity did not significantly differ between hESC-H9 and iPSC cells (**Figure 2C**). Therefore, in the remaining analysis (figures), the physiological data from the two cell lines were combined.

(A)	**Physiology**			
	hESC-H9		**iPSC-15**	
	***n* (visual fields)**	***N* (cover slips)**	***n* (visual fields)**	***N* (cover slips)**
DIV-07	4	2	0	0
DIV-08	20	2	0	0
DIV-09	8	1	6	1
DIV-10	8	2	13	2
DIV-11	7	1	3	1
DIV-14	7	1	0	0
DIV-15	6	1	8	1
DIV-16	2	1	5	1
DIV-17	6	1	9	1
DIV-18	12	2	5	2
DIV-21	2	1	5	1
Total	82	15	54	10
(B)	Gene expression analysis			
	hESC-H9	iPSC-15	Combined	
	N (cover slips)	*N* (cover slips)	*N* (cover slips)	
DIV-07	3	0	3	
DIV-08	3	0	3	
DIV-09	5	0	5	
DIV-10	1	4	5	
DIV-11	3	2	5	
DIV-12	0	2	2	
DIV-14	1	1	2	
DIV-15	2	3	5	
DIV-16	3	1	4	
DIV-17	2	2	4	
DIV-18	3	3	6	
DIV-20	1	2	3	
DIV-21	1	0	1	
Total	28	20	48	

n indicates number of visual fields used for optical recordings. Upon physiological recordings cover slips were saved for gene analysis. (B) Experimental samples used for gene analysis. These samples include cover slips saved after physiological recordings (25 cover slips in A), as well as 23 additional cover slips that were saved without any optical recordings.

Table 2. (A) Experimental samples used for physiological recordings. *N* indicates number of cover slips with cultured cells.

3.2.1. Active cells

The average percentage of cells displaying spontaneous Ca^{2+} activity increased steadily from DIV-7 through DIV-21 (**Figure 3A**). On DIV-7, the average number of active cells was 1 ± 0.1%. By DIV-14, the average number of active cells was 24 ± 4.64%, and by DIV-21, approximately 40% of cells were active (40 ± 6.3%). There was a statistically significant increase in the average percentage of active cells after the introduction of neurodifferentiation media (DIV-14 to DIV-21) as compared to that before its introduction (DIV-7 to DIV-11) ($p < 0.05$). As human neurons mature, they fire repetitive action potentials important to initiate contact with the surrounding cells [27,28]. Belinsky et al. [8] have demonstrated that repetitive activity of immature neurons can be used as a measure of their maturity.

3.2.2. Amplitude

The amplitude of spontaneous Ca^{2+} transients was analyzed over the first 3 weeks of human stem cell neurodifferentiation. Only cells with Ca^{2+} transients were included in the analysis ("Active Cells") (**Figure 2B**, upper traces). The average peak amplitude of spontaneous Ca^{2+} transients was calculated for each day in vitro (**Figure 3B**), and there was a statistically significant decrease in the average percentage of active cells after the introduction of neurodifferentiation media (DIV-14 to DIV-21) as compared to that before its introduction (DIV-8 to DIV-11) ($p < 0.05$, one-tailed *t*-test). The difference is significant when the data series DIV-8 to DIV-10 is compared to the data series DIV-11 to DIV-21 ($p < 0.05$, two-tailed *t*-test). Larger signal amplitudes were predominantly distributed in the first half of the in vitro neurodifferentiation protocol, when cell cultures primarily consisted of undifferentiated cells and neuron progenitors (**Figure 3B**).

3.2.3. Repetitive activity

Among active cells, we found a group of cells with more frequent Ca^{2+} signals (repetitive activity). The criterion for repetitive activity was set to four or more spontaneous Ca^{2+} transients in the period of time required to complete one optical recording trial (5 min). The number of cells with repetitive activity was divided by the number of active cells in the same visual field, and expressed as a percentage (**Figure 3**C). The percentage of cells exhibiting repetitive activity significantly increased with the addition of brain and glial cell-derived neurotrophic factors (BDNF and GDNF) into the cell culture media (DIV-14 to DIV- 21, as compared to DIV-7 to DIV-11; $p < 0.005$).

3.2.4. Duration

We measured the half-width (duration measured at half amplitude) of all recorded Ca^{2+} signals (n = 4726 Ca^{2+} transients obtained from 132 visual fields in 23 cover slips; DIV-7 not considered) over the first 3 weeks of human stem cell neurodifferentiation. The duration of spontaneous Ca^{2+} transients was calculated for each day of differentiation and plotted as a function of time, *day in vitro* on the *x*-axis (**Figure 3D**). The signal duration in the time period between DIV-8 to DIV-11 was significantly longer compared to the time period DIV-15 to

http://dx.doi.org/10.5772/62769

DIV-21 ($p < 0.001$). The median duration of spontaneous Ca^{2+} transients was determined to be 8 s. The Spitzer laboratory had previously reported rapid (narrow) and slow (wide) Ca^{2+} transients, but the significance of these Ca^{2+} transients at very early stages of human neurodifferentiation has as yet to be unraveled [29,30]. Based on a median duration of 8 s, we separated Ca^{2+} transients into two groups, one consisting of wide signals with duration of more than 8 s (**Figure 3E**, Wide) and the other of narrow signals with duration equal to, or less than, 8 s (**Figure 3E**, Narrow). This allowed us to calculate the percentage of narrow and wide signals at each day of differentiation (**Figure 3F**). The proportion of narrow Ca^{2+} transients increased from DIV-8 to DIV-21 (**Figure 3**F, black bars). However, at the beginning of the neurodifferentiation protocol, during Stages III and IV, the number of narrow and wide signals was about 1:1, with nearly half of the total number of Ca^{2+} transients falling into the narrow category and another half being categorized as wide. The difference between narrow and wide counts in this period (DIV-8 to DIV-11) was not statistically significant ($p < 0.05$). From DIV-15 onward, this initial balance was thrown off with narrow Ca^{2+} transients greatly outnumbering wide transients (**Figure 3F**, DIV-14 to DIV-21). There was a statistically significant difference between wide and narrow signal counts after the introduction of the differentiation factors in the culture medium, the cultures predominantly containing postmitotic neurons (DIV-14 to DIV-21), as compared to DIV-7 to DIV-11 ($p < 0.01$). Thus, the ratio of wide and narrow (less than 8 s) events can be attributed to the maturation of stem cell-derived neurons.

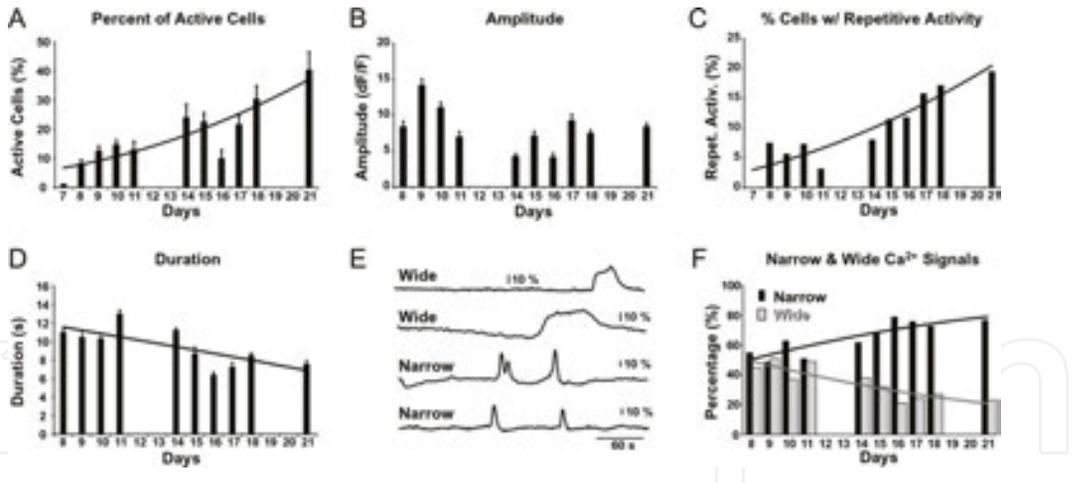

Figure 3. Spontaneous Ca^{2+}transients during early stages of neurodifferentiation. (**A**) In this and all remaining figures, the data from two cell lines are pooled together. Average number of "Active Cells" per visual field from DIV-7 to DIV-21. "Active Cells": the number of ROIs with Ca^{2+} transients divided by the total number of ROIs in that visual field (%). (**B**) Average amplitude of Ca^{2+} signals $\Delta F/F$ per day. The total number of spontaneous Ca^{2+} signals analyzed from DIV-7 to DIV-21 is 4744. (**C**) Cells with repetitive activity (4 or more Ca^{2+} transients per 5 min period) divided by the number of active cells in that visual field. An active cell is any cell with 1 or more Ca^{2+} transients per 5 min period. (**D**) Durations (half-widths) of all Ca^{2+} transients recorded in this project are plotted as average values per day. Same data set as in ***B***. (**E**) Optical traces showing wide and narrow spontaneous Ca^{2+} transients. "Wide" is defined as a signal half-width (width at half amplitude) greater than 8 s. "Narrow" is defined as a signal with half-width ≤8 s. (**F**) Distributions of Wide (gray) and Narrow (black) spontaneous Ca^{2+} transients per day, expressed as percentage of all transients on that day in vitro. Same data set as in ***D***.

Ca^{2+} release from internal stores has been reported to be especially sensitive to Ca^{2+} influx at early stages of differentiation, leading to the generation of Ca^{2+} transients of large amplitude and duration, with the sensitivity to Ca^{2+} influx decreasing as cells mature [29]. We found that larger amplitudes were predominantly distributed in the first half of our in vitro neurodifferentiation protocol, when cell cultures primarily consisted of undifferentiated cells and neuron progenitors. The amplitude of wide Ca^{2+} transients was not significantly correlated to the expression of any of the genes studied. Our results are consistent with those of Gu et al. [29]. We also observed a statistically significant positive correlation between percentage repetitive activity and the number of narrow events (action potentials; $r = 0.874$, $p < 0.001$).

The multisite Ca^{2+}imaging data indicate that spontaneous Ca^{2+} transients were present during the proliferation and differentiation phases of the in vitro neurodifferentiation protocol. The

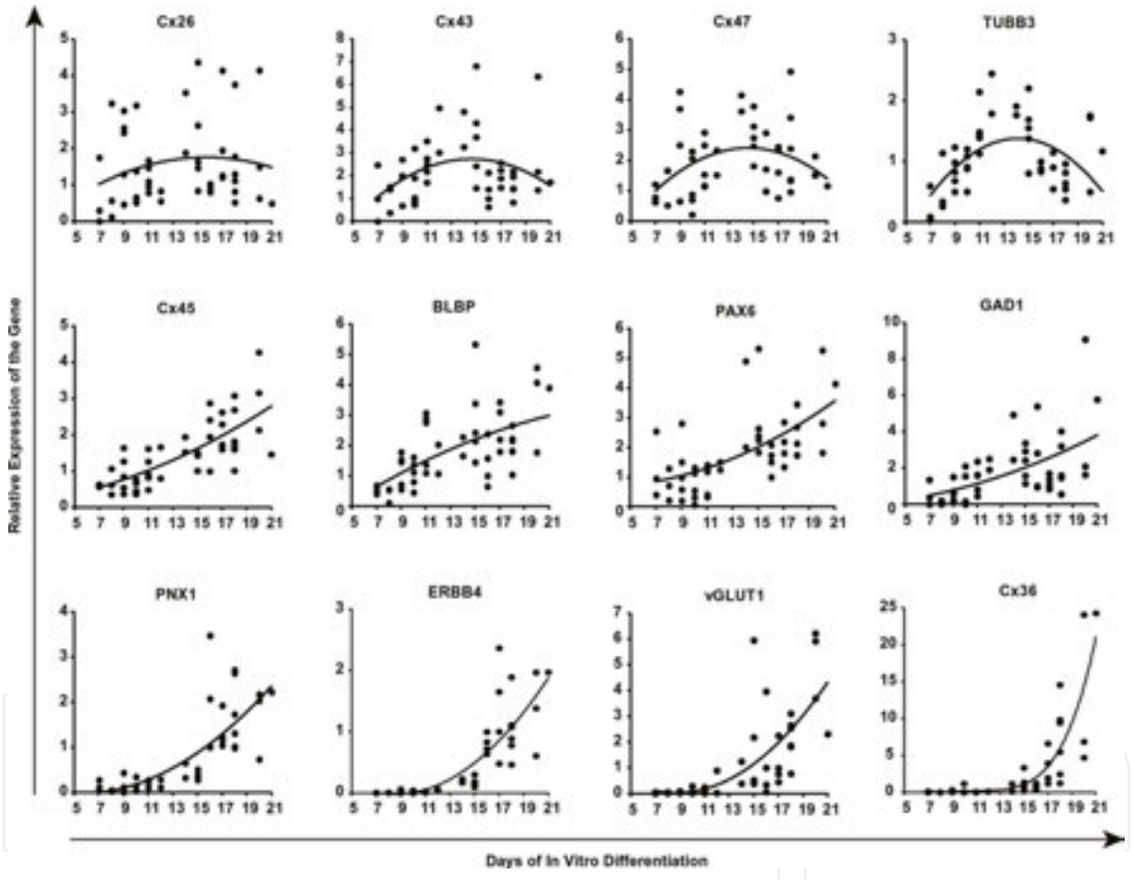

Figure 4. Gene expression levels during early stages of stem cell neurodifferentiation. The expression levels of 12 human genes (*Cx26*, *Cx43*, *Cx47*, *TUBB3*, *Cx45*, *BLBP*, *PAX6*, *GAD1*, *PNX1*, *ERBB4*, *vGLUT1*, and *Cx36*) normalized to the expression of *ACTB* over a period of 21 DIVs. Genes are organized in three rows based on the temporal patterns of expression. Top row: genes consistently expressed throughout the 21 DIVs, or with expression slowly rising and then slowly declining. Middle row: gene expression increases steadily throughout the study period (21 days). Bottom row: genes with expression starting very low and then rising exponentially as differentiation progresses. Each of the 48 data points shown in the graph represents one cover slip with cultured cells used in a qPCR reaction. *N* = number of cover slips. For DIV-7 (*N* = 3), DIV-8 (*N* = 3), DIV-9 (*N* = 5), DIV-10 (*N* = 5), DIV-11 (*N* = 5), DIV-12 (*N* = 2), DIV-14 (*N* = 2), DIV-15 (*N* = 5), DIV-16 (*N* = 4), DIV-17 (*N* = 4), DIV-18 (*N* = 6), DIV-20 (*N* = 3), and DIV-21 (*N* = 1) (**Table 2B**). The trend lines are second order polynomials, except gene *Cx36* which is fitted with a fourth order polynomial.

http://dx.doi.org/10.5772/62769

temporal patterns of three distinct parameters of Ca^{2+} transients: (a) increasing frequency, (b) decreasing peak amplitude, and (c) decreasing duration, are consistent with the gradual transition between the Ca^{2+} activities of undifferentiated cells (large amplitude–long duration) driven by a release from internal stores [17,31,32] to the spontaneous Ca^{2+} activities of postmitotic human nerve cells driven by spontaneous electrical activity [30,33,34]. The relation between electrical activity and Ca^{2+} transients in human postmitotic neurons was previously determined by simultaneous whole-cell and Ca^{2+} imaging from the same cell [8, **Figure 5**].

3.3. Gene expression during neuronal differentiation

Gene expression analysis was performed on the same biological samples in which physiological recordings were made (**Table 2A**), in order to determine if there are any correlations between gene onset, gene dynamics, and spontaneous Ca^{2+} activity. Connexin and pannexin gene isoforms are expressed in the human fetal brain at the development stages when spontaneous Ca^{2+} activity is also found [35]; these genes were analyzed in the present study along with several neuronal, glial, and human genes. More precisely, the samples were tested for four classes of genes: (1) connexins (*Cx26, Cx36, Cx43, Cx45, Cx47*, pannexin-1 (*PNX1*); (2) neuronal marker genes *PAX6, vGLUT1, GAD1, TUBB3;* (3) glial lineage markers *BLBP, GFAP*; (4) schizophrenia-associated gene (*ERBB4*). Housekeeping gene (*ACTB)* was used to normalize the gene expression values.

We compared the average expression for each of the genes, in the two cell lines, hESC-H9 and iPSC-15, over the time period DIV-7 to DIV-21 (**Table 2B**). Our gene expression results failed to detect any principal differences between the hESC-H9 and iPSC-15 cells ($p > 0.05$; $N = 28$ cover slips containing hESC-H9, and $N = 20$ cover slips with iPSC-15 cells). Our results are consistent with the single-cell PCR analysis of stem cell-derived neurons, which also found similar gene expression patterns between HESC-H9 and iPSC-15 lines [8]. Based on similar physiological (**Figure 2**C) and gene expression results (**Figure 2D**, E) obtained in two human cell lines, the data from the two cell lines were combined in the remainder of the study.

With the exception of *GFAP*, all tested genes (total number of genes tested = 14) were detected at some point between DIV-7 and DIV-21. The expression of *Cx26* was fairly constant (**Figure 4**, *Cx26*). While *Cx43, Cx47*, and *TUBB3* were upregulated in the presence of bFGF (cell proliferation stage, DIV-7 to DIV-12), their levels fell when bFGF was withdrawn on DIV-12 and differentiation factors BDNF and GDNF were added to the culture (**Figure 4**). The expression of genes *Cx45*, *BLBP*, *PAX6*, and *GAD1* did not seem to be influenced by the addition or removal of growth factors from the cell culture media (**Figure 4**). The expression of *ERBB4, Cx36*, and *vGLUT1* was negligible in the presence of bFGF (**Figure 4**), but sharply increased after the introduction of differentiation factors BDNF and GDNF to the culture medium on DIV-12.

The temporal patterns of gene expression during the course of early differentiation of human neurons were divided into four general categories (**a** – **d**) and characterized as follows:

a. Unchanging, constant expression (**Figure 5**, line "a"). The example of unchanging constant expression is the temporal pattern of *Cx26* (**Figure 4**).

b. Hyperbolic increase (**Figure 5**, line "b"). The examples of hyperbolic increase are the temporal patterns of *Cx43, Cx47*, and *TUBB3* (**Figure 4**).

c. Monotonously rising, linear increase (**Figure 5**, line "c"). The examples of linearly increasing pattern of expression are *PAX6, BLBP, Cx45*, and *GAD1* (**Figure 4**).

d. Exponential increase (**Figure 5**, "d" lines). The examples of exponentially increasing gene levels can be found in the expression patterns of *PNX1, vGLUT1, ERBB4*, and *Cx36* (**Figure 4**). An interesting aspect of the exponential increase pattern is the day of onset when gene expression becomes detectable. Our measurements showed that this day of onset varied between the genes. For example, the expression onset of *Cx36* (~DIV-17) was at least 3 days later than the onset of *ERBB4* and *vGLUT1* (~DIV-13) or 5 days later than the onset of *PNX1* (~DIV-11). Three genes, *ERBB4, vGLUT1*, and *Cx36*, exhibited their onsets after DIV-12, followed by a sharp rise in the gene expression level, suggesting that these genes responded to the addition of growth factors (GDNF and BDNF) on DIV-12.

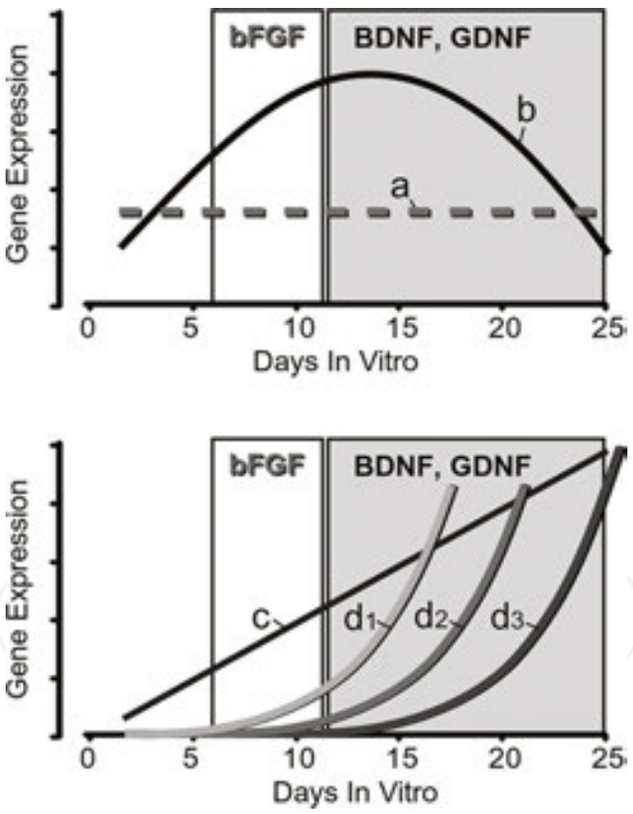

Figure 5. Characteristic patterns of gene dynamics during early stages of stem cell neurodifferentiation. Differences in differentiation media before and after DIV-12 are indicated by rectangles in the background. The four temporal patterns of gene expression levels (**a**–**d**) are based on the polynomial fits obtained from the raw data points shown in (Figure 4 (**a**) A relatively constant expression level over the entire course of differentiation for *Cx26*. (**b**) Hyperbolic pattern—a slow rise followed by a slow decline for genes *Cx43, Cx47*, and *TUBB3*. (**c**) Monotonous linear increase in the expression of *PAX6, BLBP, Cx45*, and *GAD1*. ($\mathbf{d_1}$, $\mathbf{d_2}$, and $\mathbf{d_3}$) An exponential increase with a delayed onset. The onset of the exponential rise begins on DIV-11 for *PNX1*; on DIV-13 for *ERBB4* and *vGLUT1*; and on DIV-17 for *Cx36*.

http://dx.doi.org/10.5772/62769

Next, we examined gene expression levels in relation to one significant physiological event: the onset of AP (Action Potential) firing capacity. The first APs were detected in young human neurons on DIV-14 using patch clamp recordings (**Figure 1**E). This event divides the time course of our experiment into two periods: (a) before AP firing activity was present and (b) after AP firing was established in developing human neurons. The experimental data reveals three gene expression trends in relation to the AP firing onset: (i) Negatively correlated; (ii) Unperturbed/Unrelated; and (iii) Positively correlated. In the first group "Negatively correlated", the gene expression levels were rising before AP firing was present. Upon the onset of AP firing, the gene expression trend reversed from "rising" to "falling", Three genes (*Cx43, Cx47*, and *TUBB3*) showed an apparent decline after the AP firing activity was established on DIV-14 (**Figure 4**, Top row). In the second group "Unperturbed/Unrelated", the gene expression trend did not react to the appearance of the first APs in young neurons on DIV-14. These genes are *Cx45, BLBP, PAX6, GAD1*, and *PNX1* (**Figure 4**). In the third group "Positively correlated," the gene expression was not detected before the appearance of the first APs. Following the appearance of APs on DIV-14, three genes, *ERBB4, vGLUT1*, and *Cx36*, exhibited an exponential increase in expression levels (**Figure 4**, Bottom row).

3.4. Activity to gene correlations

We next examined if there are any significant correlations between a cell's physiology, manifested through spontaneous Ca^{2+} activity, and gene expression patterns during early neuronal differentiation. Recall that the multicell calcium imaging data (**Figure 2AB**) were used to quantify the population of spontaneously active cells ("Active Cells") on a given DIV (**Figure 3A**). The same cells, in which calcium imaging was performed, were also subjected to gene analysis (**Figure 4**). This allowed us to plot physiological data and gene expression analysis data on the same graph.

3.4.1. Active cells

For example, **Figure 6A** shows similar trends of "Active Cells" (fraction of cells exhibiting spontaneous Ca^{2+} activity) and relative expression levels of the *PNX1* gene. The time course of *Cx26* expression, on the other hand, was unrelated to the fraction of cells exhibiting spontaneous Ca^{2+} activity (**Figure 6B**, "Active Cells"). We used Pearson's product–moment correlation coefficient test to study the relationship between spontaneous Ca^{2+} activity and gene expression. Two groups of genes emerged from the numerical analysis of correlation. One group of genes possessed expression patterns highly correlated with the percentage of spontaneously active cells (**Table 3**, Row: "Active Cells"; bold numbers, $p < 0.001$). This group of genes included *Cx36, BLBP, Cx45, ERBB4, GAD1, PAX6, PNX1*, and *vGLUT1*. All aforementioned genes had a positive correlation coefficient (CC), indicating that gene expression levels increased with an increase in the number of spontaneously active cells ("Active Cells"). The other group of genes exhibited expression profiles unrelated to the "Active Cells" parameter (**Table 3**, Row: "Active Cells"; pale numbers; $p > 0.001$). This group of genes included *Cx26, Cx43, TUBB3*, and *Cx47*.

(A)		*Cx26*	*Cx43*	*Cx36*	*BLBP*	*TUBB3*	*Cx45*
1	Active cells (%)	0.5651	0.1844	**0.8624**	**0.9727**	−0.0570	**0.9998**
2	Repetitive activity (%)	0.5477	0.1638	**0.8715**	**0.9677**	−0.0779	**0.9991**
3	Narrow: signal duration < 8 s; all signal amplitudes included	0.7372	0.2599	0.7244	**0.9987**	0.1152	**0.9862**
4	Moderate duration: signal duration between 8 and 20 s; signal amplitude >10%	−0.5069	**−0.8902**	0.7758	0.1590	**−0.9474**	0.3678
5	Moderate duration: signal duration between 8 and 20 s; signal amplitude > 5%	0.5534	0.0203	**0.8566**	**0.9574**	−0.1268	**0.9971**
6	Wide: signal duration > 20 s; signal amplitude < 10%	**0.8996**	**0.9935**	−0.3271	0.4146	**0.9660**	0.2090
7	Wide: signal duration > 20 s; signal amplitude > 20%	**0.9106**	**0.9902**	−0.3034	0.4380	**0.9590**	0.2343
(B)		***Cx47***	***ERBB4***	***GAD1***	***PAX6***	***PNX1***	***vGLUT1***
1	Active cells (%)	0.1641	**0.9776**	**0.99998**	**0.9994**	**0.9958**	**0.9753**
2	Repetitive activity (%)	0.1434	**0.9818**	**0.9996**	**0.9999**	**0.9975**	**0.9797**
3	Narrow: signal duration <8 s; all signal amplitudes included	0.3490	**0.8972**	**0.9634**	**0.9591**	**0.9448**	**0.9071**
4	Moderate duration: signal duration between 8 and 20 s; signal amplitude >10%	**−0.8437**	0.6190	0.4631	0.4770	0.5175	0.6008
5	Moderate duration: signal duration between 8 and 20 s; signal amplit. >5%	0.1137	**0.9770**	**0.9996**	**0.9990**	**0.9958**	**0.9817**
6	Wide: signal duration >20 s; signal amplitude <10%	**0.9998**	−0.0802	0.1055	0.0899	0.0433	−0.0573
7	Wide: signal duration >20 s; signal amplitude >20%	**0.9989**	−0.0543	0.1313	0.1157	0.0692	−0.0314

All numerical values on the right side of the table are correlation coefficients (*CC*), calculated using Pearson Product–Moment Correlation test. Bold *CC* values are statistically significant ($p < 0.001$). Pale *CC* values are not statistically significant ($p > 0.001$).

Table 3. Correlation between parameter of spontaneous calcium activity (e.g. Active Cells [%]) and normalized gene expression level (e.g. *Cx36*).

http://dx.doi.org/10.5772/62769

3.4.2. Repetitive activity

We evaluated the relation between repetitive activity and gene expression. "Repetitive Activity" is a parameter extracted from the multicell calcium imaging data. This parameter describes the number of cells in the visual field exhibiting four or more Ca^{2+} transients per 5 min of optical recording, divided by the number of "Active Cells" (cells showing at least one Ca^{2+} transient) in that field (%). We found that the same set of genes positively correlated to "Active Cells" was also positively correlated with "Repetitive Activity" (**Table 3**, Row: "Repetitive Activity").

3.4.3. Ca^{2+} signal properties

As many as 4744 spontaneous Ca^{2+} transients were documented in 25 cover slips over the period of DIV-7 to DIV-21. Each spontaneous Ca^{2+} transient was measured in terms of signal peak amplitude and signal duration (half-width), which allowed us to group data points based on signal amplitude and signal duration (**Figure 3**).

3.5. Narrow signals (<8 s)

3.5.1. GAD1 and vGLUT1

Gu and Spitzer [30] observed that the expression of the neurotransmitter GABA in developing Xenopus spinal neurons is regulated by spontaneous Ca^{2+} spikes (<5 s duration) [30]. Based on the median duration of 8 s, we categorized data points into "Narrow" and "Wide" Ca^{2+} events (**Figure 3F**). The number of *Narrow* events (<8 s) from DIV-7 to DIV-21 was significantly correlated to the expression of *GAD1* and *vGLUT1* (**Table 3**, Row 3). Since GAD1 is involved in the synthesis of GABA [17,30], these data suggest that in developing human neurons, there is a close relationship between spontaneous Ca^{2+} activity and the differentiation of neurons into GABAergic and glutamatergic neurons.

3.5.2. Cx45

The number of narrow events (with duration <8 s) was strongly ($p < 0.001$) correlated to the expression of *Cx45* (**Figure 6D**; **Table 3**, Row 3). *Cx45* is known to influence the spontaneous firing patterns in the developing retina [2].

3.5.3. BLBP

The number of narrow events (duration < 8 s) from DIV-7 to DIV-21 was significantly ($p < 0.001$) correlated to the expression of *BLBP* (**Table 3**, Row 3). BLBP expression has been reported to increase during neuronal differentiation [36], being required to induce morphological changes in radial glia in response to neuronal cues [37,38].

3.6. Wide signals (>20 s)

3.6.1. TUBB3, Cx47, and Cx26

We found that Ca^{2+} transients with duration >20 s and peak amplitude ≤10% $\Delta F/F$ not only had a strong positive correlation to the expression of the neuronal marker *TUBB3*, but also to three connexin isoforms *Cx43, Cx47*, and *Cx26* ($p < 0.001$, **Table 3**, Row 6). Connexin isoforms *Cx43* and *Cx47* were previously found in astrocytes [39,40] and oligodendrocytes [41], respectively. *Cx26* has been reported to be located on neurons and astrocytes of the developing brain as well as the leptomeninges (Nagy *et al*., 2001).

The count of Ca^{2+} transients with duration >20 s and amplitude >20% $\Delta F/F$ showed a significant positive correlation ($p < 0.001$) to the expression levels of four genes: *Cx26, Cx43, TUBB3*, and *Cx47* (**Table 3**, Rows 7). Interestingly, these were the only four genes that showed no correlation to the parameters "Active Cells" and "Repetitive Activity" (**Table 3**, Rows 1 and 2). These subsets of Ca^{2+} transients with long duration and large amplitude (duration > 20 s and amplitude > 20% $\Delta F/F$, as well as duration > 20 s and amplitude ≤ 10% $\Delta F/F$) had no significant correlation to the expression of eight genes: *Cx36, BLBP, Cx45, ERBB4, GAD1, PAX6, PNX1*, and *vGLUT1*. These are exactly the same eight genes that are highly correlated to the parameters "Active Cells" and "Repetitive Activity" (**Table 3**, Rows 1 and 2).

Overall, the correlation analyses revealed potential links between the number of cells with spontaneous calcium transients ("Active Cells" and "Repetitive Activity") and expression patterns of two connexins (*Cx36, Cx45*), one pannexin (*PNX1*), and several general neuronal genes, including *ERBB4, GAD1, PAX6*, and *vGLUT1* (**Table 3**, Rows 1 and 2). These results indicate one of two possibilities: (a) that specific subclasses of spontaneous Ca^{2+} transients could be driven by the expression of specific human genes, (b) specific amplitude and duration of Ca^{2+} transients may selectively promote expression of some human genes at early stages of neuronal differentiation. In the current study, however, we did not perform experiments to explore if expression of a certain human gene affects the incidence of spontaneous Ca^{2+} transients, with certain combinations of amplitudes and durations.

3.7. Gene-to-gene correlations

The time courses of gene expression levels shown in **Figure 4** suggest that the expression of all genes in the bottom row—*PNX1, ERBB4, vGLUT1*, and *Cx36* correlate to each other. In addition to this, we found a strong correlation ($r = 0.91$, $p < 0.001$) between *Cx43* and *TUBB3* expression (**Figure 4**, Top row).

We found that there was a statistically significant correlation between *Cx36* and *GAD1* (GABA expression; $r = 0.79$, $p < 0.01$), as well as a statistically significant correlation between *Cx36* and *vGLUT1* ($r = 0.63$, $p < 0.05$).

These data indicate that systematic sampling of gene expression levels from DIV-7 to DIV-21 during human in vitro neurodifferentiation can be used to detect groups of genes that rise and fall in parallel to each other, suggesting that their expression is driven by the same sequence of cellular and molecular events [42].

http://dx.doi.org/10.5772/62769

4. Discussion

Abnormal fetal brain development is linked to a myriad of neurological and psychiatric diseases. Human fetal gestation is a particularly sensitive stage of brain development, during which aberrant genetic programs or external factors (viruses, pollutants, toxins, and other agents) exert the most devastating impact [43,44]. The etiopathogenesis of mental illnesses, such as autism and schizophrenia, is not exclusively determined by genetic variation, but rather by the interaction of genes with the environment [45,46]. Variations in the duration and amplitude of Ca^{2+} transients and their time of occurrence affect neuronal development and plasticity [3], but these physiological aspects of human neurodifferentiation are largely absent in clinical and laboratory research. Unsurmountable ethical and technical difficulties preclude experiments on human fetuses. One possibility for studying the physiology of young human neurons is to use hESC and iPSC technologies and mimic human neurodifferentiation in vitro [6,11,47,48].

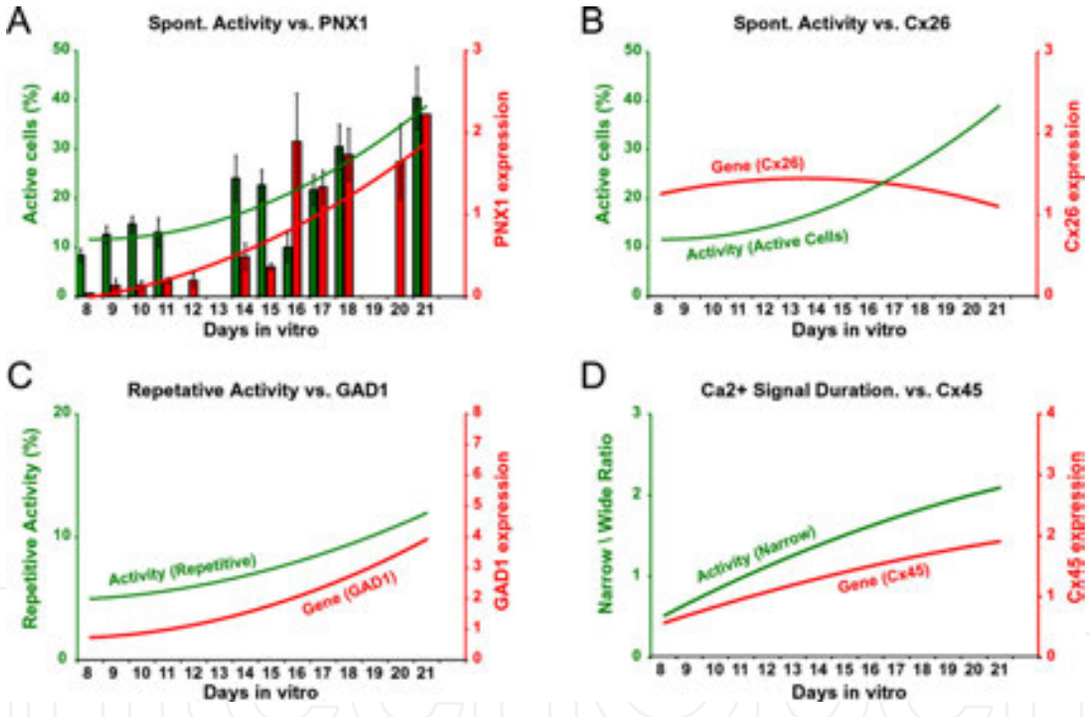

Figure 6. Correlations between different parameters of spontaneous Ca^{2+}transients and gene expression levels. (**A**) In this and all the following panels, a specific parameter of the spontaneous Ca^{2+} activity is plotted using the left ordinate axis (green), while the relative gene expression levels are plotted using the right ordinate axis (red). "Active Cells": the number of ROIs with Ca^{2+} transients divided by the total number of ROIs in that visual field (%). Each green bar represents an average value obtained on a given DIV. Each red bar represents an average relative expression of *PNX1* on a given DIV. The trend lines are polynomial fits through spontaneous Ca^{2+} activity (green) or the gene expression levels (red). The two trend lines are strongly correlated; correlation coefficient, *CC* = 0.99. (**B**) Same physiological parameter ("Active Cells") as in ***A*** is compared against the relative expression of *Cx26*. The two trend lines, physiological activity (green) and gene expression (red), are not correlated; *CC* = 0.56. (**C**) The percent of cells with repetitive Ca^{2+} activity on each day of in vitro differentiation (green) is in good correlation to the expression levels of *GAD1* (red); *CC* = 0.97. (**D**) The fraction of narrow Ca^{2+} transients on each day of in vitro differentiation (green) is positively correlated with the expression levels of *Cx45* (red); *CC* = 0.98.

In this experimental project, we have applied embryonic and pluriopotent stem cell technology to study physiological activity and gene expression during the earliest stages of human neurodifferentiation. Using multisite Ca^{2+} imaging and qPCR, we have compared time courses of spontaneous physiological Ca^{2+} activity and gene expression in two human cell lines (hESC-H9 and iPSC-15), as these cells transitioned from undifferentiated stem cells to postmitotic neurons. The iPSC-15 cell line was derived from a patient with schizo-affective disorder with a deletion on 22q11.2 that results in haploinsufficiency of ~ 40 genes, which is one of the most common causes of psychotic disorders [49–51]. We did not observe any significant differences in electrical properties, action potential frequencies, and the expression of genes important for neural development between the two cell lines, demonstrating the presence of intact cellular machinery for basic neuronal function [8].

Spontaneous Ca^{2+} transients were observed in both cell lines from the first day of recording (DIV-7), and increased in occurrence throughout the entire in vitro differentiation period. Ca^{2+} transients act via a variety of signal types, with amplitude, duration, and frequency, each encoding a specific piece of information [52]. The multisite optical imaging method used in the present study provided means for monitoring the critical parameters of Ca^{2+} transients: amplitude, duration, and frequency in up to 80 cells simultaneously. The results suggest that (a) lower amplitude, (b) greater ratio of narrow to wide signals, and (c) increased frequency are all characteristics of maturing nerve cells (**Figure 3E, F**).

4.1. Correlating spontaneous electrical activity with gene expression

Interestingly, as human cells differentiated from DIV-7 to DIV-21, there was a strong positive correlation between the number of cells exhibiting repetitive spontaneous Ca^{2+} transients and the expression levels of *GAD1* and *ERBB4* ($p < 0.001$; **Table 3**, Row 2). Also, there was a strong positive correlation ($p < 0.001$) between the number of narrow events and the expression levels of either *GAD1* or *ERBB4* (**Table 3**, Row 3). These parallel trends of *ERBB4* and *GAD1* are not surprising as GABAergic interneurons have been suggested to employ *ERBB4* receptor signaling early in the development of the cerebral cortex [53]. In accordance with our present observations, a previous study employing patch clamp recording followed by single-cell PCR revealed that individual neurons expressing *GAD1* and *ERBB4* are more likely to engage in spontaneous electrical activity than their counterparts which do not express these two genes [8]. As human cells differentiated into neurons and matured, the expression of *GAD1* and *ERBB4* increased at the same rate as the number of cells showing spontaneous Ca^{2+} activity (**Table 3**, Row 1) or the number of cells showing repetitive Ca^{2+} transients (**Figure 6C**). The regulation of the GABAergic neuronal phenotype (*GAD1* expression and production of GABA) appears to occur via an activity-dependent mechanism and is Ca^{2+}-mediated, as shown by removing extracellular Ca^{2+} or stimulating cultured neurons with different frequencies of Ca^{2+} spikes [30,54].

Narrow calcium events (Ca^{2+} transients with duration < 8 s) fit the description of AP-induced Ca^{2+} signals in postmitotic human neurons obtained by simultaneous patch clamp and optical recordings [8], and as such these short-duration Ca^{2+} signals mark the arrival of newborn neurons in stages IV and V of the current neurodifferentiation protocol (**Figure 3**F).

http://dx.doi.org/10.5772/62769

We, therefore, explored the possibility that the expression of all the other genes that correlated with repetitive activity also had a significant correlation to the number of narrow events. We found that except for *Cx36*, which is significantly correlated ($p < 0.001$) to percent repetitive activity, but not to the number of narrow events, the rest of the genes (*BLBP*, *Cx45*, *ERBB4*, *GAD1*, *PAX6*, *PNX1*, and *vGLUT1*) had a significant positive correlation to both repetitive activity and number of narrow events (**Table 3**, Rows 2 and 3). *Cx36* has been reported to be expressed during the development of retinal ganglion cells. It is thought that *Cx36* is capable of influencing spontaneous firing patterns, but is not required for spontaneous retinal wave generation [2].

The addition of growth factors BDNF and GDNF to the cell culture media appeared to have an effect on the expression of *ERBB4*, *vGLUT1*, and *Cx36*. These three genes were present at minimal levels, until the addition of growth factors on DIV-12 caused a sharp increase in their level of expression (**Figure 4**). Interestingly, the three genes showing exponential rise after DIV-14 are also highly correlated with Ca^{2+} signals of *Moderate* duration of 8–20 s and amplitude greater than 5 % $\Delta F/F$ (**Table 3**, Row 5). *Cx36* is thought to participate in neuronal gap junction formation in vivo. An increased expression of *Cx36* has been demonstrated to promote neuronal differentiation by enhancing cell–cell contact between progenitors [55]. In situ hybridization techniques have shown high levels of *Cx36* mRNA in olfactory bulbs, pineal gland, inferior olive, hippocampal pyramidal neurons, and in the retina. We found a significant correlation between *Cx36* and *GAD1* expression patterns ($r = 0.79$, $p < 0.01$), suggesting some functional link between these two genes. *Cx36* has been reported to be present on GABAergic interneurons in the neocortex and hippocampus [56]. In *Cx36*-deficient mice, gap junction-coupling among neocortical inhibitory interneurons has been shown to be nearly absent. GAD1 (GAD67) is an enzyme that synthesizes GABA and is itself influenced by Ca^{2+} signaling [17,30]. Thus, *Cx36* and *GAD1* have a close relationship, which may be a part of the regulatory mechanisms for expression of GABA and/or GABAergic interneuron differentiation.

In addition to having a significant correlation to *GAD1*, we found that there was a significant correlation between *Cx36* and the *vGLUT1* expression patterns ($r = 0.63$, $p < 0.05$) over the period DIV-8 to DIV-21. The *Cx36* gene has been reported to be induced at the time of the surge of the transcription factors that determine β-cell differentiation [57]. Thus, during neuronal differentiation, *Cx36* could potentially influence transcription factors that determine the terminal differentiation of neurons to either glutamatergic or GABAergic, with the *Cx36* channels forming intercellular pathways for transmission of developmentally relevant molecules. Upregulation of *Cx36* expression has also been previously associated with the sequential expression of specific ligand-gated responses (GABA and glutamate), thus heralding terminal differentiation of neurons, with the peak expression of *Cx36* being associated with a developmental window in which the neuronal network connections are being developed [58].

In the present study, we found that *Cx43*, *Cx47*, and *TUBB3* showed a hyperbolic pattern of expression, wherein there was an upregulation of these genes during the cell proliferation stage (in the presence of the proliferation factor bFGF) and a subsequent decrease in their

expression. Both the increase and the decrease of *Cx43*, *Cx47*, and *TUBB3*, relative to the characteristic time periods of the differentiation protocol (e.g. replacement of proliferation media on DIV-12; appearance of first APs on DIV-14; sharp onset of *Cx36* expression on DIV-17), may become useful for understanding the roles of these three genes in human neurodifferentiation.

We found that the decline of *TUBB3* after DIV-14 was paralleled by an upregulation of *GAD1* (putative GABAergic neurons) and *vGLUT1* (putative glutamatergic neurons) during the differentiation phase (**Figure 4**, compare *TUBB3, GAD1*, and *vGLUT1*). Similar to our results, a decrease in the expression of the neuronal progenitor marker *TUBB3* along with a simultaneous increase in GABA and glutamatergic neurons during neuronal differentiation was also observed by [42]. We found a strong correlation between *Cx43* and *TUBB3* expression ($r = 0.91$, $p < 0.001$), which suggests a close relationship between *Cx43* expression on astrocytes and *TUBB3* expression on neuronal progenitors. *Cx43* is essential for the maintenance of neural progenitors in a proliferative state [59, 60] and forms communication channels, between migrating neurons and the glial cells, during neurogenesis [61].

By sampling data points on consecutive days (DIV-7 to DIV-21), we observed that the expression of human *GAD1* occurred before the expression of human *vGLUT1* (**Figure 4**), as has been reported in the literature, where the formation of GABAergic synapses in the CNS preceded that of glutamatergic synapses [62]. In summary, as cells exit from the cell cycle and undergo lineage commitment, as shown by the expression of *ERBB4, GAD1*, and *vGLUT1*, they demonstrate a changing profile of connexin expression with *Cx43* and *Cx47* declining, *Cx45* and *PNX1* increasing, and *Cx36* being activated.

Although *BLBP* was expressed in our cell culture, *GFAP* was not expressed at detectable levels. Both *GFAP* and *BLBP* are expressed on radial glia during early neuronal development, but their expression has been reported to be nonoverlapping [63]. In line with our experimental results, *GFAP* was observed to be expressed only after the expression of *BLBP* during in vitro culture of human embryonic stem cells [42]. Thus, culturing cells for a period longer than 21 days is necessary for observing *GFAP* expression.

When correlation analysis was performed between Ca^{2+} transients with specific characteristics of duration and amplitude, and the expression of specific genes involved in neurodifferentiation, we observed that specific subclasses of Ca^{2+} transients are linked to specific genes. Two possible scenarios can explain the observed positive correlations between spontaneous physiological activity and gene expression. First, specific calcium transients could be driven by the expression of specific human genes. Second, one type of calcium transients (e.g., short duration and small amplitude) may selectively influence the expression of some but not all human genes during early neuronal development.

Spike stimulation mimicking the frequency of spontaneous transients has been shown to be most effective in replicating the effects of spontaneous transients on neurotransmitter expression, for example, GABA expression [30,54]. Thus, it would be quite useful to find calcium spike properties (amplitude, duration, and frequencies) that promote the expression

http://dx.doi.org/10.5772/62769

of genes involved in early neuronal differentiation in order to improve current methods for modeling human brain development in culture.

Acknowledgements

This study was supported by Connecticut Innovations grant 09-SCA-UCHC-13 to SDA, NIH grants MH063503 and MH104775 to SDA, HCRAC Institutional grant to SDA, and NIH grants MH087840 and MH099427 to HML. Electrophysiological and optical measurements were performed in the *Stem Cell Physiology and Chemistry Core*, which is supported by Connecticut Innovations grant SCD-01-2009 to SDA. The LED-based epi-illumination system was designed and built by Dr. Peter Lee, Essel R&D Inc., Toronto, Canada. The authors are grateful to Drs. Steven Crocker and Richard Mains (UConn Health) for help with the qPCR apparatus.

Author contributions

Designed the study: GSB and SDA. Produced iPSCs: EP and HML. Stem cell neurodifferentiation: GSB, PVL, and MLM. Patch electrode recordings and multisite calcium imaging: MBS, KDO, and SDA. Gene expression levels: PVL, GSB, and MLM. Analyzed the experimental data: PVL, MLM, MBS, and SDA. Wrote the paper: PVL, HML, and SDA.

Competing interests

The authors have declared that no competing interests exist.

Author details

Pallavi V. Limaye[1], Michele L. McGovern[1], Mandakini B. Singh[1], Katerina D. Oikonomou[1], Glenn S. Belinsky[1], Erika Pedrosa[2], Herbert M. Lachman[2] and Srdjan D. Antic[1*]

*Address all correspondence to: antic@uchc.edu

1 Stem Cell Institute, Institute for Systems Genomics, UConn Health, Farmington, CT, USA

2 Department of Psychiatry and Behavioral Sciences, Albert Einstein College of Medicine, Bronx, New York, USA

References

[1] Moody, W.J. and M.M. Bosma (2005) *Ion channel development, spontaneous activity, and activity-dependent development in nerve and muscle cells*. Physiol Rev, 85(3): p. 883–941.

[2] Blankenship, A.G. and M.B. Feller (2011) *Mechanisms underlying spontaneous patterned activity in developing neural circuits*. Nat Rev Neurosci, 11(1): p. 18–29.

[3] Rosenberg, S.S. and N.C. Spitzer (2011) *Calcium signaling in neuronal development*. Cold Spring Harb Perspect Biol, 3(10): p. a004259.

[4] Moore, A.R., R. Filipovic, Z. Mo, M.N. Rasband, N. Zecevic, and S.D. Antic (2009) *Electrical excitability of early neurons in the human cerebral cortex during the second trimester of gestation*. Cereb Cortex, 19(8): p. 1795–805.

[5] Moore, A.R., W.L. Zhou, I. Jakovcevski, N. Zecevic, and S.D. Antic (2011) *Spontaneous electrical activity in the human fetal cortex in vitro*. J Neurosci, 31(7): p. 2391–8.

[6] Belinsky, G.S., A.R. Moore, S.M. Short, M.T. Rich, and S.D. Antic (2011) *Physiological properties of neurons derived from human embryonic stem cells using a dibutyryl cyclic AMP-based protocol*. Stem Cells Dev, 20(10): p. 1733–46.

[7] Chatzidaki, A., A. Fouillet, J. Li, J. Dage, N.S. Millar, E. Sher, and D. Ursu (2015) *Pharmacological characterisation of nicotinic acetylcholine receptors expressed in human iPSC-derived neurons*. PLoS One, 10(4): p. e0125116.

[8] Belinsky, G.S., M.T. Rich, C.L. Sirois, S.M. Short, E. Pedrosa, H.M. Lachman, and S.D. Antic (2014) *Patch-clamp recordings and calcium imaging followed by single-cell PCR reveal the developmental profile of 13 genes in iPSC-derived human neurons*. Stem Cell Res, 12(1): p. 101–18.

[9] Preynat-Seauve, O., D.M. Suter, D. Tirefort, L. Turchi, T. Virolle, H. Chneiweiss, M. Foti, J.A. Lobrinus, L. Stoppini, A. Feki, M. Dubois-Dauphin, and K.H. Krause (2009) *Development of human nervous tissue upon differentiation of embryonic stem cells in three-dimensional culture*. Stem Cells, 27(3): p. 509–20.

[10] Ma, L., Y. Liu, and S.C. Zhang (2011) *Directed differentiation of dopamine neurons from human pluripotent stem cells*. Methods Mol Biol, 767: p. 411–8.

[11] Liu, H., J. Lu, H. Chen, Z. Du, X.J. Li, and S.C. Zhang (2015) *Spinal muscular atrophy patient-derived motor neurons exhibit hyperexcitability*. Sci Rep, 5: p. 12189.

[12] Pre, D., M.W. Nestor, A.A. Sproul, S. Jacob, P. Koppensteiner, V. Chinchalongporn, M. Zimmer, A. Yamamoto, S.A. Noggle, and O. Arancio (2014) *A time course analysis of the electrophysiological properties of neurons differentiated from human induced pluripotent stem cells (iPSCs)*. PLoS One, 9(7): p. e103418.

[13] Brennand, K.J. and F.H. Gage (2011) *Concise review: the promise of human induced pluripotent stem cell-based studies of schizophrenia*. Stem Cells, 29(12): p. 1915–22.

[14] Chamberlain, S.J., P.F. Chen, K.Y. Ng, F. Bourgois-Rocha, F. Lemtiri-Chlieh, E.S. Levine, and M. Lalande (2010) *Induced pluripotent stem cell models of the genomic imprinting disorders Angelman and Prader–Willi syndromes*. Proc Natl Acad Sci U S A, 107(41): p. 17668–73.

[15] Zhao, D., M. Lin, J. Chen, E. Pedrosa, A. Hrabovsky, H.M. Fourcade, D. Zheng, and H.M. Lachman (2015) *MicroRNA profiling of neurons generated using induced pluripotent stem cells derived from patients with schizophrenia and schizoaffective disorder, and 22q11.2 del*. PLoS One, 10(7): p. e0132387.

[16] Rowe, E.W., D.M. Jeftinija, K. Jeftinija, and S. Jeftinija (2005) *Development of functional neurons from postnatal stem cells in vitro*. Stem Cells, 23(8): p. 1044–9.

[17] Holliday, J., R.J. Adams, T.J. Sejnowski, and N.C. Spitzer (1991) *Calcium-induced release of calcium regulates differentiation of cultured spinal neurons*. Neuron, 7(5): p. 787–96.

[18] Hill, E.J., C. Jimenez-Gonzalez, M. Tarczyluk, D.A. Nagel, M.D. Coleman, and H.R. Parri (2012) *NT2 derived neuronal and astrocytic network signalling*. PLoS One, 7(5): p. e36098.

[19] Tonelli, F.M., A.K. Santos, D.A. Gomes, S.L. da Silva, K.N. Gomes, L.O. Ladeira, and R.R. Resende (2012) *Stem cells and calcium signaling*. Adv Exp Med Biol, 740: p. 891–916.

[20] Konur, S. and A. Ghosh (2005) *Calcium signaling and the control of dendritic development*. Neuron, 46(3): p. 401–5.

[21] Rosenberg, S.S. and N.C. Spitzer (2011) *Calcium signaling in neuronal development*. Cold Spring Harb Perspect Biol., 3(10): p. a004259.

[22] Yamamoto, N. and G. Lopez-Bendito (2012) *Shaping brain connections through spontaneous neural activity*. Eur J Neurosci, 35(10): p. 1595–604.

[23] Uhlen, P. and N. Fritz (2010) *Biochemistry of calcium oscillations*. Biochem Biophys Res Commun, 396(1): p. 28–32.

[24] Pedrosa, E., V. Sandler, A. Shah, R. Carroll, C. Chang, S. Rockowitz, X. Guo, D. Zheng, and H.M. Lachman (2011) *Development of patient-specific neurons in schizophrenia using induced pluripotent stem cells*. J Neurogenet, 25(3): p. 88–103.

[25] Iacovitti, L., A.E. Donaldson, C.E. Marshall, S. Suon, and M. Yang (2007) *A protocol for the differentiation of human embryonic stem cells into dopaminergic neurons using only chemically defined human additives: studies in vitro and in vivo*. Brain Res, 1127(1): p. 19–25.

[26] Zeng, H., M. Guo, K. Martins-Taylor, X.F. Wang, Z. Zhang, J.W. Park, S.N. Zhan, M.S. Kronenberg, A. Lichtler, H.X. Liu, F.P. Chen, L.X. Yue, X.J. Li, and R.H. Xu (2010) *Specification of region-specific neurons including forebrain glutamatergic neurons from human induced pluripotent stem cells*. PLos One, 5(7): p. e11853.

[27] Price, D.J., H. Kennedy, C. Dehay, L. Zhou, M. Mercier, Y. Jossin, A.M. Goffinet, F. Tissir, D. Blakey, and Z. Molnar (2006) *The development of cortical connections*. Eur J Neurosci, 23(4): p. 910–20.

[28] Bando, Y., K. Irie, T. Shimomura, H. Umeshima, Y. Kushida, M. Kengaku, Y. Fujiyoshi, T. Hirano, and Y. Tagawa (2014) *Control of spontaneous Ca^{2+} transients is critical for neuronal maturation in the developing neocortex*. Cereb Cortex, 26(1): p. 106–17.

[29] Gu, X., E.C. Olson, and N.C. Spitzer (1994) *Spontaneous neuronal calcium spikes and waves during early differentiation*. J Neurosci, 14(11 Pt 1): p. 6325–35.

[30] Gu, X. and N.C. Spitzer (1995) *Distinct aspects of neuronal differentiation encoded by frequency of spontaneous Ca^{2+} transients*. Nature, 375(6534): p. 784–7.

[31] Leclerc, C., I. Neant, S.E. Webb, A.L. Miller, and M. Moreau (2006) *Calcium transients and calcium signalling during early neurogenesis in the amphibian embryo Xenopus laevis*. Biochim Biophys Acta, 1763(11): p. 1184–91.

[32] Resende, R.R., J.L. da Costa, A.H. Kihara, A. Adhikari, and E. Lorencon (2010) *Intracellular Ca^{2+} regulation during neuronal differentiation of murine embryonal carcinoma and mesenchymal stem cells*. Stem Cells Dev, 19(3): p. 379–94.

[33] Malmersjo, S., P. Rebellato, E. Smedler, H. Planert, S. Kanatani, I. Liste, E. Nanou, H. Sunner, S. Abdelhady, S. Zhang, M. Andang, A. El Manira, G. Silberberg, E. Arenas, and P. Uhlen (2013) *Neural progenitors organize in small-world networks to promote cell proliferation*. Proc Natl Acad Sci U S A, 110(16): p. E1524–32.

[34] Conhaim, J., C.R. Easton, M.I. Becker, M. Barahimi, E.R. Cedarbaum, J.G. Moore, L.F. Mather, S. Dabagh, D.J. Minter, S.P. Moen, and W.J. Moody (2011) *Developmental changes in propagation patterns and transmitter dependence of waves of spontaneous activity in the mouse cerebral cortex*. J Physiol, 589(Pt 10): p. 2529–41.

[35] Moore, A.R., W.L. Zhou, C.L. Sirois, G.S. Belinsky, N. Zecevic, and S.D. Antic (2014) *Connexin hemichannels contribute to spontaneous electrical activity in the human fetal cortex*. Proc Natl Acad Sci U S A, 111(37): p. E3919–28.

[36] Retrosi, G., N.J. Sebire, M. Bishay, E.M. Kiely, J. Anderson, P. De Coppi, E. Resca, D. Rampling, N. Bier, K. Mills, S. Eaton, and A. Pierro (2011) *Brain lipid-binding protein: a marker of differentiation in neuroblastic tumors*. J Pediatr Surg, 46(6): p. 1197–200.

[37] Feng, L., M.E. Hatten, and N. Heintz (1994) *Brain lipid-binding protein (BLBP): a novel signaling system in the developing mammalian CNS*. Neuron, 12(4): p. 895–908.

[38] Anton, E.S., M.A. Marchionni, K.F. Lee, and P. Rakic (1997) *Role of GGF/neuregulin signaling in interactions between migrating neurons and radial glia in the developing cerebral cortex*. Development, 124(18): p. 3501–10.

[39] Nagy, J.I., D. Patel, P.A. Ochalski, and G.L. Stelmack (1999) *Connexin30 in rodent, cat and human brain: selective expression in gray matter astrocytes, co-localization with connexin43 at gap junctions and late developmental appearance*. Neuroscience, 88(2): p. 447–68.

[40] Nadarajah, B., A.M. Jones, W.H. Evans, and J.G. Parnavelas (1997) *Differential expression of connexins during neocortical development and neuronal circuit formation*. J Neurosci, 17(9): p. 3096–111.

[41] Odermatt, B., K. Wellershaus, A. Wallraff, G. Seifert, J. Degen, C. Euwens, B. Fuss, H. Bussow, K. Schilling, C. Steinhauser, and K. Willecke (2003) *Connexin 47 (Cx47)-deficient mice with enhanced green fluorescent protein reporter gene reveal predominant oligodendrocytic expression of Cx47 and display vacuolized myelin in the CNS*. J Neurosci, 23(11): p. 4549–59.

[42] Taléns-Visconti, R., I. Sanchez-Vera, J. Kostic, M.A. Perez-Arago, S. Erceg, M. Stojkovic, and C. Guerri (2011) *Neural differentiation from human embryonic stem cells as a tool to study early brain development and the neuroteratogenic effects of ethanol*. Stem Cells Dev, 20(2): p. 327–39.

[43] Lewis, D.A. and P. Levitt (2002) *Schizophrenia as a disorder of neurodevelopment*. Annu Rev Neurosci, 25: p. 409–32.

[44] Rapoport, J.L., A.M. Addington, S. Frangou, and M.R. Psych (2005) *The neurodevelopmental model of schizophrenia: update 2005*. Mol Psychiatry, 10(5): p. 434–49.

[45] Matelski, L. and J. Van de Water (2015) *Risk factors in autism: thinking outside the brain*. J Autoimmun, 67: p. 1–7.

[46] Owen, M.J., A. Sawa, and P.B. Mortensen (2016) *Schizophrenia*. Lancet, pii: S0140℃6736(15): p. 01121–6.

[47] Brennand, K.J., A. Simone, J. Jou, C. Gelboin-Burkhart, N. Tran, S. Sangar, Y. Li, Y. Mu, G. Chen, D. Yu, S. McCarthy, J. Sebat, and F.H. Gage (2011) *Modelling schizophrenia using human induced pluripotent stem cells*. Nature, 473(7346): p. 221–5.

[48] Suzuki, M., A.D. Nelson, J.B. Eickstaedt, K. Wallace, L.S. Wright, and C.N. Svendsen (2006) *Glutamate enhances proliferation and neurogenesis in human neural progenitor cell cultures derived from the fetal cortex*. Eur J Neurosci, 24(3): p. 645–53.

[49] Lin, M., H.M. Lachman, and D. Zheng (2015) *Transcriptomics analysis of iPSC-derived neurons and modeling of neuropsychiatric disorders*. Mol Cell Neurosci, pii: S1044–7431(15): p. 30035–X.

[50] Meechan, D.W., T.M. Maynard, E.S. Tucker, and A.S. LaMantia (2011) *Three phases of DiGeorge/22q11 deletion syndrome pathogenesis during brain development: patterning, proliferation, and mitochondrial functions of 22q11 genes*. Int J Dev Neurosci, 29(3): p. 283–94.

[51] Shprintzen, R.J., A.M. Higgins, K. Antshel, W. Fremont, N. Roizen, and W. Kates (2005) *Velo-cardio-facial syndrome*. Curr Opin Pediatr, 17(6): p. 725–30.

[52] Parekh, A.B. and S. Muallem (2011) *Ca(2+) signalling and gene regulation*. Cell Calcium, 49(5): p. 279.

[53] Mei, L. and W.C. Xiong (2008) *Neuregulin 1 in neural development, synaptic plasticity and schizophrenia*. Nat Rev Neurosci, 9(6): p. 437–52.

[54] Watt, S.D., X. Gu, R.D. Smith, and N.C. Spitzer (2000) *Specific frequencies of spontaneous Ca^{2+} transients upregulate GAD 67 transcripts in embryonic spinal neurons*. Mol Cell Neurosci, 16(4): p. 376–87.

[55] Hartfield, E.M., F. Rinaldi, C.P. Glover, L.F. Wong, M.A. Caldwell, and J.B. Uney (2011) *Connexin 36 expression regulates neuronal differentiation from neural progenitor cells*. PLoS One, 6(3): p. e14746.

[56] Thompson, R.J. and B.A. Macvicar (2008) *Connexin and pannexin hemichannels of neurons and astrocytes*. Channels (Austin), 2(2): p. 81–6.

[57] Nlend, R.N., A. Ait-Lounis, F. Allagnat, V. Cigliola, A. Charollais, W. Reith, J.A. Haefliger, and P. Meda (2012) *Cx36 is a target of Beta2/NeuroD1, which associates with prenatal differentiation of insulin-producing beta cells*. J Membr Biol, 245(5–6): p. 263–73.

[58] Rozental, R., C. Giaume, and D.C. Spray (2000) *Gap junctions in the nervous system*. Brain Res Brain Res Rev, 32(1): p. 11–15.

[59] Duval, N., D. Gomes, V. Calaora, A. Calabrese, P. Meda, and R. Bruzzone (2002) *Cell coupling and Cx43 expression in embryonic mouse neural progenitor cells*. J Cell Sci, 115(Pt 16): p. 3241–51.

[60] Cheng, A., H. Tang, J. Cai, M. Zhu, X. Zhang, M. Rao, and M.P. Mattson (2004) *Gap junctional communication is required to maintain mouse cortical neural progenitor cells in a proliferative state*. Dev Biol, 272(1): p. 203–16.

[61] Montoro, R.J. and R. Yuste (2004) *Gap junctions in developing neocortex: a review*. Brain Res Brain Res Rev, 47(1–3): p. 216–26.

[62] Ben-Ari, Y. (2002) *Excitatory actions of GABA during development: the nature of the nurture*. Nat Rev Neurosci, 3(9): p. 728–39.

[63] Howard, B., Y. Chen, and N. Zecevic (2006) *Cortical progenitor cells in the developing human telencephalon*. Glia, 53(1): p. 57–66.